



**Direct Inhibition of the First PDZ Domain of ZO-1 by
Glycyrrhizin is a Possible Mechanism of Tight Junction
Opening of Caco-2 Cells.**

Journal:	<i>Food & Function</i>
Manuscript ID	FO-ART-09-2021-003062.R1
Article Type:	Paper
Date Submitted by the Author:	08-Dec-2021
Complete List of Authors:	Hibino, Emi; Nagoya Univerisity Goda, Natsuko; Nagoya Univerisity Hisada, Misaki; Nagoya Univerisity Tenno, Takeshi; Nagoya Univerisity Hiroaki, Hidekazu; Nagoya Univerisity,

Title

Direct Inhibition of the First PDZ Domain of ZO-1 by Glycyrrhizin is a Possible Mechanism of Tight Junction Opening of Caco-2 Cells.

Authors

Emi Hibino¹, Natsuko Goda¹, Misaki Hisada¹, Takeshi Tenno^{1,2}, and Hidekazu Hiroaki^{1,2,*}.

¹Laboratory of Structural Molecular Pharmacology, Graduate School of Pharmaceutical Sciences, Nagoya University, Furocho, Chikusa-ku, Nagoya, Aichi, Japan, 464-8601.

²BeCellBar LLC., Business Incubation Building, Nagoya University, Furocho, Chikusa-ku, Nagoya, Aichi, Japan, 464-8601.

Abstract

Glycyrrhizin (GL) is known to exhibit a variety of useful pharmacological activities, including anti-inflammation, anti-hepatotoxicity, and enhancement of intestinal drug absorption. GL has been reported to modify the assembly of actin filaments, thereby modulating tight junction (TJ) integrity, but the detailed molecular mechanisms of this remain unclear. In this study, we first found that GL binds to the first PDZ domain of zonula occludens-1 (ZO-1(PDZ1)) through NMR experiments. The structure of the GL–ZO-1(PDZ1) complex was then constructed using HADDOCK with the transferred nuclear Overhauser effect-based inter-hydrogen distance constraints as well as restrictions on the interfacial residues identified from ¹H-¹⁵N HSQC spectral changes. We identified the relevant interactions between the glucuronate-2 moiety of GL and the carboxylate binding loop of the ligand binding site of ZO-1(PDZ1). We further examined the interaction of ZO-1(PDZ1) with glycyrrhetic acid and with GA-3-monoglucuronide

and observed a much lower affinity for each than for that of GL, with good agreement to the model. The other contacts found in the model were examined by using an amino acid substitution mutant of ZO-1(PDZ1). Finally, we reproduced the experiments reported by Sakai *et al.* in which high-dose GL prolonged the TJ-opening mediated with sodium deoxycholate as indicated by reduced trans-epithelial electrical resistance. (204 words)

1. Introduction

Glycyrrhizin (GL) is a triterpene glycoside and the principal active ingredient in the medicinal herb liquorice (*Glycyrrhiza glabra*).^{1,2} GL exhibits variety beneficial pharmacological activities, including anti-inflammation and anti-hepatotoxicity. These activities of GL can be explained through the inhibition of the extracellular high-mobility group box-1 (HMGB1) protein. The secreted form of HMGB1 is known to act as a pro-inflammatory cytokine.³ For example, in endothelial cells, HMGB1 disrupts vascular barrier function by modulating the expression of several intercellular adhesion molecules.⁴ One of the major physiological receptors for HMGB1 is the receptor for advanced glycation end-products (RAGE). GL directly binds to HMGB1 and prevents its binding to RAGE⁵ as well as to DNA.⁶

Another reported beneficial function of GL is in its application as an intestinal drug absorption enhancer.^{7,8} Although GL alone cannot alter the epithelial permeability of the Caco-2 cell monolayer, it prolongs the tight junction (TJ) loosening activity of both sodium deoxycholate (DCA) and capric acid when GL is administrated either of these simultaneously. While researchers have observed that GL modifies the assembly of TJ-associated actin filaments followed by an alteration in TJ-integrity, the detailed molecular mechanisms remain unclear.⁷

TJs are composed of four-transmembrane spanning proteins called claudins (CLDs) and occludin, and the cytosolic scaffold proteins called zonula occludens (ZO)-1/2/3.^{9–11} The molecular functions of these ZO proteins are thought to connect and stabilize CLDs using their three tandem postsynaptic density-95/discs large/ZO-1 (PDZ) domains in corroboration with the dimerization and actin-binding domains.^{12,13} Among these three PDZ domains of ZO-1 (and its close paralog ZO-2), the first PDZ domain is the interface responsible for recognizing the C-terminal PDZ-binding motifs (PBMs) of CLDs.¹⁴ This specific interaction between CLD C-termini and ZO-1 plays a crucial role in TJ biogenesis and the maintenance of their integrity.¹⁵ For example, ZO-1 knockout/ZO-2 knockdown resulted in loss of CLDs organization in TJ area.¹⁶ Similarly, the cells of ZO-1 and ZO-2 double knockdown exhibited decreased some (but not all) CLDs localization at TJ area with abnormal accumulation of apical actin.¹⁷ Accordingly, the mutations in the PBMs of CLDs have shown to result in defective phenotypes.¹⁸ We have previously reported that several compounds that directly bind to the first PDZ domain of ZO-1 (ZO-1(PDZ1)) can loosen TJs.^{19–22} Based on these facts, we hypothesized that GL also directly binds to ZO-1(PDZ1), prolonging the TJ-opening activity of known absorption enhancers, capric acid and DCA.

In this study, we first performed NMR titration experiments on ¹⁵N-labelled ZO-1(PDZ1) with GL. Several chemical shift perturbations (CSPs) were observed and mapped around the residues corresponding to the canonical CLD-binding cleft of ZO-1(PDZ1). We also observed cross peaks from the transferred nuclear Overhauser effect (trNOE) among the protons of GL in the presence of ZO-1(PDZ1). These inter-hydrogen distance constraints and data on interfacial residues derived by the CSPs were analysed to derive the GL–ZO-1(PDZ1) complex structure. We identified the indispensable interactions within the complex structure, which were then further confirmed by NMR

experiments using GL analogues, glycyrrhetic acid (GA) and GA-3-mono-glucuronide (GAMG), as well as an amino acid substitution mutant of ZO-1(PDZ1). We also succeeded in reproducing the experiments reported by Sakai *et al.*,⁷ where a high-dose of GL prolonged the decreased trans-epithelial electric resistance (TEER) initiated by DCA.

2. Materials and methods

2.1 Protein expression and purification

The preparation of ZO-1(PDZ1) and V82E/R86Q mutant was performed as described previously.²³ Briefly, the protein was expressed in *Escherichia coli* BL21(DE3) grown in M9 minimal medium culture containing [¹⁵N]-NH₄Cl or LB medium under isopropyl-β-D-1-thiogalactopyranoside (IPTG) induction. The supernatant of the sonicated cells was purified using DEAE Sepharose (Cytiva, Marlborough, MA, USA) and Glutathione Sepharose 4 Fast Flow (Cytiva). After the cleavage of GST-tag by PreScission protease (Cytiva) at 4°C, the protein was further purified using size exclusion chromatography with a Superdex 75 HR 26/60 column (Cytiva) equilibrated with 20 mM Tris-HCl (pH 7.5 at 4°C) and 150 mM NaCl. The purified proteins were concentrated and dialyzed with 22 mM MES (pH 6.5).

2.2 NMR Experiments

The NMR experiments were performed on a Bruker Avance III (600 MHz and 900 MHz) NMR spectrometer (Bruker, Karlsruhe, Germany) equipped with a cryogenic triple-resonance probe. For the NMR titration experiments, the protein concentration was 100 μM in a solution that contained 20 mM MES (pH 5.9), 5% (v/v) D₂O, and DMSO-*d*₆ (Isotec Inc., USA), where each compound was dissolved and ¹H-¹⁵N HSQC spectra were obtained. The DMSO-*d*₆ in which the compound was dissolved was prepared to contain 4% in the NMR sample. GL (TCI, Tokyo, Japan) was added at 50, 75, 100, and 150 μM,

and GA (TCI), GA 3-*O*-glucuronide (TCI), and glucuronic acid were added at 200 μM , respectively. The amide resonance assignments for ZO-1(PDZ1) have already been published.²³ Chemical shift change ($\Delta\delta_{\text{H,N}}$) was calculated with the following equation (1);

$$\Delta\delta_{\text{H,N}} = \sqrt{(\Delta\delta_{\text{H}})^2 + (\Delta\delta_{\text{N}}/5)^2} \quad (1)$$

where $\Delta\delta_{\text{H}}$ and $\Delta\delta_{\text{N}}$ are the chemical shift differences in the presence and absence of the compound, respectively. The concentration of GL was plotted on the horizontal axis against $\Delta\delta_{\text{H,N}}$ on the vertical axis and fitted to obtain the dissociation constant (K_{d}) with the following equation (2);

$$\Delta\delta_{\text{H,N}} = \Delta\delta_{\text{max}} \times \frac{([\text{Pt}] + [\text{Lt}] + K_{\text{d}}) - \sqrt{([\text{Pt}] + [\text{Lt}] + K_{\text{d}})^2 - 4[\text{Pt}] \times [\text{Lt}]}}{2 \times [\text{Pt}]} \quad (2)$$

where $[\text{Lt}]$ and $[\text{Pt}]$ are the concentration of GL and ZO-1(PDZ1), respectively, and $\Delta\delta_{\text{max}}$ is $\Delta\delta_{\text{H,N}}$ in the case of moving to the maximum, and $\Delta\delta_{\text{max}}$ and K_{d} were calculated by fitting using Igor 8.04 software.

For the trNOE experiments, the GL was 2 mM and unlabelled ZO-1(PDZ1) was 40 μM in 93% (v/v) D_2O buffer containing 20 mM phosphate, pH5.9. The $\text{DMSO-}d_6$ in which the compound was dissolved was prepared to contain 2% (v/v) in the NMR sample. All samples contained dimethyl-2-silapentane-5-sulfonate as an internal reference. The ^1H - ^1H NOESY spectra were obtained with 150 ms and 500 ms mixing time. To assign the ^1H - ^1H NOESY spectra, the ^1H - ^{13}C HSQC spectrum of 2 mM free GL in 93% (v/v) D_2O buffer containing 20 mM phosphate and 2% (v/v) $\text{DMSO-}d_6$, pH5.9 was used. The assignment of the ^1H - ^{13}C HSQC spectrum of the GL was obtained from the published ^1H spectrum of GL.²⁴ All spectra were processed and analysed using the SPARKY program.²⁵

2.3 Computational docking

The GL and ZO-1(PDZ1) complex structures were obtained using the HADDOCK 2.4 program.²⁶ For the structure of ZO-1(PDZ1), we used the NMR structures already published and registered to the Protein Data Bank (PDB),²³ and the PDB code is 2RRM. We used all 20 structures registered in 2RRM. The GL structure was generated using Avogadro software²⁷ and PyMOL software.²⁸ The distance of the hydrogens in the bound state of GL was calculated from the trNOE experiments. Mixing time was taken as the horizontal axis and peak intensity as the vertical axis, and a straight line passing through the origin was fitted by Igor 8.04 software. The distance of 5H and 9H was obtained from the distance measurement tool of PyMOL. The distances between the assigned atoms were calculated based on 5H and 9H NOE peak intensities and distances using equations (3) and (4);

$$I = \sigma \times t_m \quad (3)$$

where I is peak intensity, t_m is mixing time, and σ was calculated;

$$r = (A/\sigma)^{1/6} \quad (4)$$

where r is the distance between hydrogen atoms, and A is a proportion coefficient. The calculated r was used as a constraint through the HADDOCK simulation. The residues of ZO-1(PDZ1) that were significantly altered in the NMR titration experiments were defined as the binding sites of ZO-1(PDZ1).

For comparison, we also calculated two HADDOCK structures, one with no restrictions and the other with only the CSP data as a restriction.

2.4 Cell culture

The Caco-2 cells were cultured in Minimum Essential Medium Eagle (Sigma-Aldrich, St Louis, MO, USA) supplemented with 10% FBS (Biosera, Boussens, France), 1% penicillin/streptomycin (Gibco, Paisley, UK), and 1% MEM-NEAA (Gibco) at 37 °C with 5% CO₂.

2.5 Measurement of trans-epithelial electrical resistance (TEER)

We measured TEER as described previously.²⁹ Briefly, the Caco-2 cells were cultured to a tight monolayer on an upper transwell filter and maintained for approximately 14 days until stable TEER was achieved. The TEER of the cell monolayer was measured with an epithelial volt-ohmmeter (Millicell® ERS-2; Merck-Millipore, Billerica, MA, USA). The TEER was measured before administration of the compound and then 1, 3, and 24 hours after administration, and every 24 hours thereafter until 144 hours.

3. Results

3.1 NMR evidence of direct binding of GL to ZO-1(PDZ1)

ZO-1 is a peripheral membrane phosphoprotein located on the cytoplasmic side and is expressed in the TJs of both epithelial and endothelial cells, forming an intercellular barrier. ZO-1 consists of the three PDZ domains as well as the SH3 domain, GK domain, and ZU5 domain (Fig.1A). ZO-1(PDZ1) binds to the C-terminal PBMs of almost all CLDs, leading to the formation of TJs.¹⁵ We found that ZO-1(PDZ1) binds to GL through the following NMR experiments. A comparison of the ¹H-¹⁵N HSQC spectra of 100 μM ¹⁵N-ZO-1(PDZ1) in the absence and the presence of 150 μM GL revealed many CSPs (Fig.1B).

To investigate the residues that contribute to GL-binding, we then analysed these CSPs against the residue numbers from previously reported assignments for ZO-1(PDZ1) (Fig. 1C).²³ Since the CSPs were observed in only a limited number of residues, we were confident that the overall structure of ZO-1(PDZ1) was retained upon GL-binding. In detail, we found that the signals corresponding to Ala29, Gly33, Phe34, Gly35,

Ala37, Gly99, and Lys100 showed marked CSPs. We mapped these residues onto the solution structure of ZO-1(PDZ1) (PDB: 2RRM).²⁰ It was obvious that GL-binding occurred at the region including $\alpha 1$ and $\beta 2$ in the PDZ domain, which spatially overlapped the canonical binding pocket (Fig. 1D). The binding pocket of the PDZ domain typically recognizes the C-terminal of the last four residues of the physiological ligand of the corresponding PDZ proteins. Since GL's chemical structure is completely different from that of the peptide, it was surprising that GL, a triterpenoid with two glucuronate moieties, had bound directly to ZO-1(PDZ1).

3.2 TrNOE experiment.

Although the HSQC spectrum led us to identify that the amino acid residues of ZO-1(PDZ1) that interacted with the GL, the molecular recognition mechanism of GL by ZO-1(PDZ1) remained unclear. We decided to determine the complex structure of GL–ZO-1(PDZ1) based on NMR-derived experimental information. For this purpose, we employed inter-proton distance restraints that reflected the bound state conformation of GL to ZO-1(PDZ1) for accurate model building. Therefore, we measured the trNOE. It is widely known that the use of a rigid single conformation of ligands can contribute to accurate docking experiments.³⁰ We set the concentrations of GL and ZO-1(PDZ1) to 2 mM and 40 μ M, respectively. Under these conditions, the ZO-1(PDZ1) concentration corresponds to 1/50 of the amount of GL. The measurement of the trNOE was performed using standard ^1H - ^1H NOESY experiments with a mixing time of either 150 ms or 500 ms (Fig. 2A, B). In the results, several cross peaks were observed, which were further assigned based on the chemical shift of the ^1H signals. We measured a natural abundance of the 2D ^1H - ^{13}C HSQC spectra of the GL, and all of the GL signals were identified based on the literature with a slight modification (Fig. 2C and Fig. S1A).²⁴ The mixing-time dependence according to the growth of the intensities of the trNOE signals was analysed,

and then interpreted as the inter-proton distances from the slope of the line toward the origin. Accordingly, the intensity of the trNOE peak between 5H and 7H of the GL, whose distance is fixed, was used as the internal reference of the inter-proton distance for interpreting the trNOE data (Fig. S1B). All these values and the estimated inter-proton distances of the ZO-1(PDZ1)-bound state conformation of GL are summarized in Table S1.

It should be noted that GL is an amphiphilic molecule and is reported to form micelles at higher concentrations, and we carefully confirmed ruling out the influence of micelle formation in our trNOE experiment. At pH 5.9 and 25°C, which were the conditions of the ^1H - ^{15}N HSQC measurements, we measured the ^1H - ^1H NOESY spectra of GL alone (without the ZO-1(PDZ1)) at the conformation of either 2 mM or 4mM. We found the peak intensity of 4 mM GL was smaller than that of 2 mM GL. Since peak intensity should normally increase depending on concentration, we concluded that micelles were formed at 4 mM, whereas micelles of GL were not formed at 2 mM. We also concluded that GL exists as a monomer up to at least 2 mM (Fig. S2). In other words, GL most likely exists as a monomer at the condition of our trNOE experiments.

3.3 Determination of the GL–ZO-1(PDZ1) complex structure by HADDOCK

We then calculated the complex structure model of GL and ZO-1(PDZ1) by using the HADDOCK 2.4 program (Fig. 3A, B and Table S2).²⁶ The structure of apo-ZO-1(PDZ1) was taken from an NMR structure reported previously (PDB, 2RRM).²³ The restrictions of the interfacial residues of ZO-1(PDZ1) to GL were applied during the docking calculation based on the NMR titration experiments. In addition, the intramolecular inter-proton distance constraints of the GL molecule were applied. We succeeded in obtaining a complex structure in a good agreement with the NMR data. In

the complex structure, the GL molecule was kinked at its two glycoside-bonds and adopted into an L-shaped conformation (Fig. 3A). The GL molecule covered over half of the canonical peptide binding pocket of the PDZ domain, around the carboxylate-binding ('GLGF') loop and $\alpha 2$ - $\beta 5$ loop, while the rest of the pocket near the $\beta 2$ - $\beta 3$ loop was still vacant. We found two critical hydrogen bonds between the carboxyl group of the glucuronate-2 moiety and the main-chain amides of Phe34 and Gly35 of ZO-1(PDZ1). The rest of the glucuronate-2 moiety was further recognized by two additional residues, Phe32 and Ile36. In addition, the aglycone of GL and the main chain of Arg28 and Gly31 formed hydrogen bonds. Glucuronate-1 was additionally recognized by the side chain of Arg96.

We further assessed whether this docking structure was valid by mutually omitting the experimental datasets during calculation. We calculated the complex structure with only the restrictions of the interfacial residues but without the trNOE-based interproton restraints and also without any of the restrictions (Fig. S3 and Table S2). In these cases, we still succeeded in building complex models in which the GL molecule covered over the canonical ligand binding pocket between $\beta 2$ and $\alpha 1$. However, we concluded that these models were less consistent with our experimental data because the two glucuronate moieties did not face the ZO-1(PDZ1). Since PDZ domains are modular functional domains dedicated to recognizing the C-terminal residues of membrane proteins, we initially expected that one of the three carboxyl groups of GL would mimic the C-terminus of CLDs. Surprisingly, the HADDOCK docking achieved the formation of hydrogen bonds between the GLGF-loop and the carboxyl-group of the second glucuronate residue only when the trNOE derived constraints were applied (Fig. S3D, E).

3.4 Experimental validation of the relevant interactions found in the GL-ZO-1(PDZ1) model.

As described above, the docking model suggested several relevant molecular interactions, mainly hydrogen bonds, between GL and ZO-1(PDZ1). Thus, we examined the existence and relevance of these atomic contacts through NMR experiments using GL analogues and a ZO-1(PDZ1) mutant. We first compared the ^1H - ^{15}N HSQC spectra of ZO-1(PDZ1) in the absence and the presence of two GL analogues, GA (Fig. S4A, C), GAMG (Fig. 4), and glucuronic acid (Fig. S4B, D). Note that GA is the aglycone of GL without glucuronate moieties (Fig. S4A), whereas GAMG is lacking the glucuronate-2 moiety of GL (Fig. 4A). Glucuronic acid was used as a negative control without the aglycone of GL (Fig. S4B). As expected, we only observed weak CSPs even upon the addition of two molecular equivalents of GAMG, while there were no CSPs with GA or glucuronic acid (Fig. 4B and Fig. S4C, D). Thus, among them, we found that GAMG had a residual affinity that was rather weaker than that of GL (Fig. 4C). Based on these observations, we concluded that the two glucuronate moieties are relevant for GL-ZO-1(PDZ1) recognition.

Next, we also validated the contribution of the sidechain of the important residues which were found by the HADDOCK-derived GL-ZO-1(PDZ1) complex structure. For this purpose, we prepared for this experiment by mutating the side chains involved in binding. In the HADDOCK structure, we focused on the side chain of Arg96, which was involved in the GL-binding. In addition, we found that the side chain of Val92 was attaching Arg96 and supporting the direction of the side chain of Arg96 towards GL. Since the CSP of Arg96 was not significant in the GL-binding experiment, we prepared the double mutant V92E/R96Q. The ^1H - ^{15}N HSQC spectra of the ZO-1(PDZ1) V92E/R96Q mutant at a concentration of 100 μM were measured in the absence and

presence of 1.5 equivalents of GL (Fig. 5). As expected, the chemical shift changes upon the addition of GL were significantly small, suggesting the importance of the binding pocket formed by the side chains of Arg96 and Val92 in GL-binding. This result also supported the idea that the GL was directly binding to the binding pocket of the ZO-1(PDZ1).

3.5 Determination of the dissociation constant K_d from the NMR experiments.

Next, we determined the dissociation constant of GL to ZO-1(PDZ1) from the NMR titration experiment. To prepare the saturation curve upon GL-binding, we measured the HSQC spectra of the ZO-1(PDZ1) in the presence of 50, 75, 100, and 150 μM of GL, which correspond to 0.5, 0.75, 1, and 1.5 molecular equivalents of ZO-1(PDZ1), respectively (Fig. 6). We gave up on measuring the HSQC spectra with the over 1.5 equivalents of GL because additions of GL exceeding 1.5 equivalents resulted in a slight precipitation. The seven residues with marked CSPs were chosen and plotted against the GL concentrations, and the saturation curves were fitted by the equation (See experimental procedures) (Fig. 6B). The calculated dissociation constant K_d was $266 \pm 141 \mu\text{M}$. It should be noted that K_d for the C-terminal peptide of CLD2, one of the typical physiological ligands of ZO-1(PDZ1), was $13.5 \pm 1.3 (\mu\text{M})$. Since the difference in the K_d value between the GL and CLD2 against the ZO-1(PDZ1) was of only one order, we assumed that a high concentration of GL can interfere with the physiological interaction between ZO-1 and CLDs.

3.6 Pharmacological activity of GL and its analogues against the TEER of the Caco-2 cell monolayer.

As described above, based on our in vitro experiments, we hypothesized that GL incorporates into the cytosol at a high enough concentration. Nevertheless, several lines of experiments showed that GL alone did not affect the TJ-integrity of the Caco-2 cell monolayer as estimated by TEER measurement.^{7,8} Instead, the GL was reported to enhance or prolong the TJ-loosening activities of the other drug excipients, either DCA⁷ or capric acid.⁸ Thus, in this study, we intended to reproduce the co-administration experiment using GL and DCA according to the study by Sakai *et al.*,⁷ and we also examined the effect of GAMG, a GL analogue.

The Caco-2 cells were cultured for more than two weeks until TEER reached a plateau prior to the experiments. TEER was measured before and after 1, 3, 24, 48, 72, 96, 120, and 144 hours of the treatment (Fig. S5A). As shown in Fig. S5B, TEER with GL or GAMG alone did not show any differences with the negative control. First, we compared the rate of change in TEER with GL or GAMG with that of the negative control and found no significant difference (Fig. S5B). The results were consistent with the already reported GL activity and also consistent with the fact that the bioavailability and intercellular penetration of GL are believed to be low. Since GL is a glycoside with two glucuronate moieties, Lipinski's drug-likeness parameter is too far from the rule of five, and it is assumed to have merely penetrated across the cell membrane. In contrast, when GL was co-administrated with DCA, the decreased TEER was kept almost all the time (Fig. S5C). We assumed that this result was due to cell damage caused by long-term administration of DCA and GL. Accordingly, we changed the administration time course of the DCA with GL or GAMG, and DCA was applied for only the first 60 minutes, whereas GL or GAMG was continuously administrated (Fig. 7A). Comparing the single-pulse treatment of DCA alone with the co-administration of GL with DCA, the co-administered GL showed a marked prolonged decrease in TEER over 36 hours longer

than that of with only the administration of DCA at the first dose, suggesting a sustained TJ-opening. In order to examine the effect of GL without DCA, GL or DMSO was administered after the second dose. The TEER profile was similar in both cases, indicating that GL is not effective without DCA. These results seem consistent with our expectation that GL acts against some cytosolic targets to keep TJs open after GL has permeated across the cell membrane (Fig. 7B). The TJ-loosening activity of GAMG was comparable to that of GL.

4. Discussion

The present study has demonstrated the direct binding of GL to ZO-1(PDZ1) and the details of the molecular recognition mechanisms in the NMR-derived GL–ZO-1(PDZ1) complex structure. To build a more reliable complex model, we employed a trNOE for GL in the presence of ZO-1(PDZ1). We succeeded in obtaining the complex structure of GL–ZO-1(PDZ1) with a HADDOCK calculation by using two independent NMR-derived constraints, intramolecular inter-proton distances among the GL molecule from the trNOE, and restrictions of the interfacial residues of ZO-1(PDZ1) as defined by the CSPs upon GL-binding. The complex structure was calculated by docking simulations using the results of the trNOE and NMR titration experiments as constraints, and the structure was validated by additional NMR experiments. The complex structure was further assessed by additional NMR binding experiments using either of two GL analogues lacking one or two glucuronate moieties, GAMG and GA, respectively, or using the ZO-1(PDZ1) mutant V92E/R96Q. In both experiments, since the binding affinity decreased reasonably, we concluded that the obtained complex model reached a reasonable accuracy. We observed a unique trNOE cross peak with a medium intensity between H1 in the GA moiety of GL and H2' of the glucuronate-1 moiety. Reflecting this constraint, GL adopted a unique L-shaped conformation in the complex structure, which

is unique to ZO-1(PDZ1) recognition. Without the trNOE derived constraints, the GL molecule tends to adopt into an elongated conformation (Fig. S3C-E). It is assumed that the L-shaped bound conformation of GL is different from the most stable conformation of free GL in an aqueous solution, which may hamper tight GL–ZO-1(PDZ1) interaction because of enthalpic loss. This L-shaped conformation also seems different from the HMGB1-bound state of GL, although the precise coordinates have not yet been published.⁵

The GL–ZO-1(PDZ1) complex model allowed us to discuss the detailed interaction mechanism between GL and the PDZ domain. Since PDZ domains are modular functional domains dedicated to recognizing the C-terminal residues of membrane proteins, we initially expected that one of the three carboxyl groups of GL would mimic the C-terminus of CLDs. The crystal structure of the CLD1–ZO-1(PDZ1) complex has revealed that the important residues involved in the recognition of CLD1 by ZO-1(PDZ1) are Phe34 and Gly35.¹⁴ Strikingly, we found that the carboxyl group of the glucuronate-2 moiety was also recognized by the same residues in a similar coordination. Nevertheless, the binding modes of these two molecules are rather different. The N-terminal half of the CLD1 peptide was located along the peptide binding cleft sandwiched by $\alpha 2$ and $\beta 3$ and continuously in contact with the $\beta 2$ - $\beta 3$ loop. In contrast, the GA moiety of GL was kinked and covered the surface of the $\beta 1$ - $\beta 2$ loop and $\alpha 2$ - $\beta 5$ loop. Thus, although the binding sites spatially overlapped between the CLD1 peptide and GL, the combination of interaction residues was rather different. The involvement of the glucuronate-2 moiety in ZO-1(PDZ1) recognition is also unique as compared to its binding to HMGB1. It should be noted that not only GL but also GA can bind HMGB1, while ZO-1 can bind specifically to GL but only weakly to GAMG and GA.

Interestingly, GL did not affect the integrity of the TJs of the Caco-2 cell monolayer when administrated alone. DCA is one of the surfactants found in bile, and bile salts are known as drug absorption enhancers via the paracellular transport of other substances.^{31–33} Recently, the improved bioavailability of GL with DCA/phospholipid nanomicelles has been reported.³⁴ However, some reports have also demonstrated that bile salts enhance the transcellular transport of drugs across cell membranes.³⁵ We assumed that GL permeated into the cytosol of the Caco-2 cells with the help of DCA despite that the large molecular weight of GL with two glucuronate moieties is not ideal for cell membrane permeation. We hypothesized that the target molecule of the prolonged TJ-opening activity of GL is a cytosolic factor related to the TJ-regulatory pathways, including of transcription, biogenesis, maintenance, and degradation. Since we observed the direct binding of GL to ZO-1(PDZ1), we propose that the inhibition of ZO-1 function by GL is one of the mechanisms of the prolonged TJ-opening by GL in a similar manner to that of other TJ-opening substances or compounds, such as phosphatidylinositol phosphates,²⁰ baicalin,²¹ quercetin,²⁹ diclofenac, and indomethacin.²²

The NMR titration experiments revealed that GL binds to ZO-1(PDZ1) at $K_d = 266 \mu\text{M}$. In contrast, although the affinity of GAMG to ZO-1(PDZ1) is rather weak, its TJ-loosening activity was comparable to GL. To explain this phenomenon, we consider the following three possibilities: (1) the bioavailability of GAMG is higher than that of GL, and the high intracellular concentration of GAMG was able to overcome its weaker affinity against ZO-1(PDZ1), (2) GAMG was further metabolized after cell uptake and glucuronidated in conversion to GL, and (3) there should be other TJ-opening pathways, including the protein kinase C (PKC) pathway, and GAMG may act against this alternative pathways more efficiently than GL. Note that Sakai *et al.* further showed that cytosolic GL (or its metabolite) may modulate actin cytoskeleton via activation of the

PKC through not-yet-identified cytosolic target molecules.⁷ However, they also showed that the contribution of the PKC cascade was only partial as treatment with PKC inhibitor H7 failed to recover the DCA/GL-induced TEER decrease. These possibilities will be studied further in the future.

Based on GL's pharmacological activity, ectopic HMGB1 has been one of the most studied targets for GL as an anti-inflammatory drug.⁵ The reported K_d of GL to HMGB1 is approximately 150 μM . GA, the aglycone of GL, was also reported to bind HMGB1. Since HMGB1 acts as a pro-inflammatory cytokine via the RAGE/ERK signalling pathway,³⁶ its influence on TJs is essentially through the loosening and/or down-regulation of TJ components. Thus, under pro-inflammatory or inflammatory conditions, it is reasonable to state that the administration of GL may possibly ameliorate TJ dysfunction in many different epithelial cell types via inhibition of HMGB1 (Fig. 8B).³⁷⁻³⁹ In contrast, we demonstrated GL's TJ-opening activity, which is apparently in opposition to its reported protective function (Fig. 8A). Based on these results, we hypothesize that the TJ-opening by GL co-administrated with DCA is attributable to the different pharmacological action of GL as a HMGB1 inhibitor. Based on our NMR studies of the molecular recognition of GL by ZO-1(PDZ1), we propose that one of the candidates for the cytosolic target of GL is ZO-1.

5. Conclusion

In this work, we propose the direct inhibition of ZO-1, which is the major TJ-organizer, is an additional mechanism of the action by GL in the TJ-loosening of Caco-2 cell monolayers. Accordingly, we assume that the co-administration of surfactants, such as DCA, with GL may accelerate the cellular uptake of GL as GL alone has

difficulty entering cells except in a specific organ case in which the cells are expressing asialoglycoprotein receptors. The action of DCA is still our working hypothesis, and this should be studied further. Since DCA and GL are both relatively safe compounds, the co-administration of DCA and GL is an ideal prescription for drug absorption enhancement.

Conflicts of interest

Among the authors, T.T. and H.H. are the founders of a Nagoya University-based spinoff startup company BeCellBar LLC. The other authors declare that they have no conflicts of interest in the contents of this article.

Author Contributions

Conceptualization, E.H., N.G., T.T., and H.H.; investigation, E.H., N.G., M.H., and T.T.; data curation, E.H., N.G., T.T., and H.H.; resources, N.G and T.T.; formal analysis, E.H.; visualization, E.H.; writing-original draft, E.H. and H.H.; writing-review and editing, E.H. and H.H.; supervision, H.H.; project administration, H.H.; funding acquisition, H.H. All authors have read and agreed to the published version of this manuscript.

Acknowledgements

This work was supported in part by the Japan Science and Technology Agency, A-step Feasibility Study Program (AS262Z01275Q, AS242Z00566Q), Japan Society for the Promotion of Science KAKENHI (15H04337), AMED Translational Research Program,

and Strategic PRomotion for practical application of INnovative medical Technology (TR-SPRINT) under Grant Number 201m0203011-j0002.

The authors would like to thank Scribendi Editing Services (<https://www.scribendi.com/>) for the English language review.

Abbreviations

GL (glycyrrhizin), TJ (tight junction), ZO (zonula occludens), GA (glycyrrhetic acid), GAMG (glycyrrhetic acid-3-monoglucuronide), HMGB1 (high-mobility group box-1), RAGE (receptor for advanced glycation end-products), DCA (sodium deoxycholate), CLDs (claudins), PBMs (PDZ-binding motifs), CSPs (chemical shift perturbations), trNOE (transferred nuclear Overhauser effect), TEER (trans-epithelial electric resistance), PKC (protein kinase C), PDB (Protein Data Bank)

Footnotes

This article contains supplementary information.

References

- 1 M. N. Asl and H. Hosseinzadeh, Review of Pharmacological Effects of Glycyrrhiza sp. and its Bioactive Compounds, *Phyther. Res.*, 2008, **22**, 709–724.
- 2 S. Shibata, A Drug over the Millennia: Pharmacognosy, Chemistry, and Pharmacology of Licorice, *Yakugaku Zasshi*, 2000, **120**, 849–862.
- 3 M. T. Lotze and K. J. Tracey, High-mobility group box 1 protein (HMGB1): Nuclear weapon in the immune arsenal, *Nat. Rev. Immunol.*, 2005, **5**, 331–342.
- 4 M. I. Nawaz and G. Mohammad, Role of high-mobility group box-1 protein in disruption of vascular barriers and regulation of leukocyte–endothelial interactions, *J. Recept. Signal Transduct.*, 2015, **35**, 340–345.
- 5 L. Mollica, F. De Marchis, A. Spitaleri, C. Dallacosta, D. Pennacchini, M. Zamai, A. Agresti, L. Trisciuglio, G. Musco and M. E. Bianchi, Glycyrrhizin Binds to High-Mobility Group Box 1 Protein and Inhibits Its Cytokine Activities, *Chem. Biol.*, 2007, **14**, 431–441.
- 6 R. Sakamoto, M. Okano, H. Takena and K. Ohtsuki, Inhibitory effect of glycyrrhizin on the phosphorylation and DNA-binding abilities of high mobility group proteins 1 and 2 in vitro, *Biol. Pharm. Bull.*, 2001, **24**, 906–911.
- 7 M. Sakai, T. Imai, H. Ohtake, H. Azuma and M. Otagiri, Simultaneous Use of Sodium Deoxycholate and Dipotassium Glycyrrhizinate Enhances the Cellular

- Transport of Poorly Absorbed Compounds Across Caco-2 Cell Monolayers, *J. Pharm. Pharmacol.*, 1999, **51**, 27–33.
- 8 T. Imai, M. Sakai, H. Ohtake, H. Azuma and M. Otagiri, Absorption-enhancing effect of glycyrrhizin induced in the presence of capric acid, *Int. J. Pharm.*, 2005, **294**, 11–21.
- 9 M. S. Balda and K. Matter, Transmembrane proteins of tight junctions, *Semin. Cell Dev. Biol.*, 2000, **11**, 281–289.
- 10 S. Aijaz, M. S. Balda and K. Matter, Tight junctions: Molecular architecture and function, *Int. Rev. Cytol.*, 2006, **248**, 261–298.
- 11 H. Chiba, M. Osanai, M. Murata, T. Kojima and N. Sawada, Transmembrane proteins of tight junctions, *Biochim. Biophys. Acta - Biomembr.*, 2008, **1778**, 588–600.
- 12 L. González-Mariscal, A. Betanzos, P. Nava and B. E. Jaramillo, Tight junction proteins, *Prog. Biophys. Mol. Biol.*, 2003, **81**, 1–44.
- 13 C. M. Van Itallie, A. J. Tietgens and J. M. Anderson, Visualizing the dynamic coupling of claudin strands to the actin cytoskeleton through ZO-1, *Mol. Biol. Cell*, 2017, **28**, 524–534.
- 14 J. Nomme, A. Antanasijevic, M. Caffrey, C. M. Van Itallie, J. M. Anderson, A. S. Fanning and A. Lavie, Structural basis of a key factor regulating the affinity between the zonula occludens first PDZ domain and claudins, *J. Biol. Chem.*, 2015, **290**, 16595–16606.
- 15 M. Itoh, M. Furuse, K. Morita, K. Kubota, M. Saitou and S. Tsukita, Direct binding of three tight junction-associated MAGUKs, ZO-1, ZO-2, and ZO-3, with the COOH termini of claudins, *J. Cell Biol.*, 1999, **147**, 1351–1363.
- 16 K. Umeda, J. Ikenouchi, S. Katahira-Tayama, K. Furuse, H. Sasaki, M. Nakayama, T. Matsui, S. Tsukita, M. Furuse and S. Tsukita, ZO-1 and ZO-2 Independently Determine Where Claudins Are Polymerized in Tight-Junction Strand Formation, *Cell*, 2006, **126**, 741–754.
- 17 A. S. Fanning, C. M. Van Itallie and J. M. Anderson, Zonula occludens-1 and -2 regulate apical cell structure and the zonula adherens cytoskeleton in polarized epithelia, *Mol. Biol. Cell*, 2012, **23**, 577–590.
- 18 M. Furuse, Knockout animals and natural mutations as experimental and diagnostic tool for studying tight junction functions in vivo, *Biochim. Biophys. Acta*, 2009, **1788**, 813–819.
- 19 T. Tenno, N. Goda, Y. Umetsu, M. Ota, K. Kinoshita and H. Hiroaki, Accidental interaction between PDZ domains and diclofenac revealed by NMR-assisted virtual screening, *Molecules*, 2013, **18**, 9567–9581.
- 20 H. Hiroaki, K. Satomura, N. Goda, Y. Nakakura, M. Hiranuma, T. Tenno, D. Hamada and T. Ikegami, Spatial overlap of claudin- and phosphatidylinositol phosphate-binding sites on the first PDZ domain of zonula occludens 1 studied by NMR, *Molecules*, 2018, **23**, 2465.
- 21 M. Hisada, M. Hiranuma, M. Nakashima, N. Goda, T. Tenno and H. Hiroaki, High dose of baicalin or baicalein can reduce tight junction integrity by partly targeting the first PDZ domain of zonula occludens-1 (ZO-1), *Eur. J. Pharmacol.*, 2020, **887**, 173436.
- 22 T. Tenno, K. Kataoka, N. Goda and H. Hiroaki, Nmr-guided repositioning of non-steroidal anti-inflammatory drugs into tight junction modulators, *Int. J. Mol. Sci.*, 2021, **22**, 1–17.
- 23 Y. Umetsu, N. Goda, R. Taniguchi, K. Satomura, T. Ikegami, M. Furuse and H. Hiroaki, ¹H, ¹³C, and ¹⁵N resonance assignment of the first PDZ domain of mouse ZO-1, *Biomol. NMR Assign.*, 2011, **5**, 207–210.
- 24 V. Sai, P. Chaturvedula, O. Yu and G. Mao, NMR Analysis and Hydrolysis Studies of Glycyrrhizic Acid, a Major Constituent of Glycyrrhiza Glabra, *Chem. Bull*, 2014, **3**, 104–107.

- 25 W. Lee, M. Tonelli and J. L. Markley, NMRFAM-SPARKY: Enhanced software for biomolecular NMR spectroscopy, *Bioinformatics*, 2015, **31**, 1325–1327.
- 26 G. C. P. Van Zundert, J. P. G. L. M. Rodrigues, M. Trellet, C. Schmitz, P. L. Kastiris, E. Karaca, A. S. J. Melquiond, M. Van Dijk, S. J. De Vries and A. M. J. J. Bonvin, The HADDOCK2.2 Web Server: User-Friendly Integrative Modeling of Biomolecular Complexes, *J. Mol. Biol.*, 2016, **428**, 720–725.
- 27 M. D. Hanwell, D. E. Curtis, D. C. Lonie, T. Vandermeersch, E. Zurek and G. R. Hutchison, Avogadro: an advanced semantic chemical editor, visualization, and analysis platform, *J. Cheminform.*, 2012, **4**, 17.
- 28 L. Schrödinger, 2015.
- 29 M. Nakashima, M. Hisada, N. Goda, T. Tenno, A. Kotake, Y. Inotsume, I. Kameoka and H. Hiroaki, Opposing effect of naringenin and quercetin on the junctional compartment of mdck ii cells to modulate the tight junction, *Nutrients*, 2020, **12**, 1–17.
- 30 S. Mukherjee, T. E. Balias and R. C. Rizzo, Docking validation resources: Protein family and ligand flexibility experiments, *J. Chem. Inf. Model.*, 2010, **50**, 1986–2000.
- 31 Y. J. Lin and W. C. Shen, Effects of Deoxycholate on the Transepithelial Transport of Sucrose and Horseradish Peroxidase in Filter-Grown Madin–Darby Canine Kidney (MDCK) Cells, *Pharm. Res.*, 1991, **8**, 498–501.
- 32 M. Sakai, T. Imai, H. Ohtake, H. Azuma and M. Otagiri, Effects of absorption enhancers on the transport of model compounds in Caco-2 cell monolayers: Assessment by confocal laser scanning microscopy, *J. Pharm. Sci.*, 1997, **86**, 779–785.
- 33 Y. L. Lo and J.-D. Huang, Effects of sodium deoxycholate and sodium caprate on the transport of epirubicin in human intestinal epithelial Caco-2 cell layers and everted gut sacs of rats, *Biochem. Pharmacol.*, 2000, **59**, 665–672.
- 34 S. Jin, S. Fu, J. Han, S. Jin, Q. Lv, Y. Lu, J. Qi, W. Wu and H. Yuan, Improvement of oral bioavailability of glycyrrhizin by sodium deoxycholate/phospholipid-mixed nanomicelles, *J. Drug Target.*, 2012, **20**, 615–622.
- 35 K. Kim, I. Yoon, I. Chun, N. Lee, T. Kim and H. S. Gwak, Effects of bile salts on the lovastatin pharmacokinetics following oral administration to rats, *Drug Deliv.*, 2011, **18**, 79–83.
- 36 C. Ott, K. Jacobs, E. Haucke, A. Navarrete Santos, T. Grune and A. Simm, Role of advanced glycation end products in cellular signaling, *Redox Biol.*, 2014, **2**, 411–429.
- 37 S. H. Lee, I. H. Bae, H. Choi, H. W. Choi, S. Oh, P. A. Marinho, D. J. Min, D. Y. Kim, T. R. Lee, C. S. Lee and J. Lee, Ameliorating effect of dipotassium glycyrrhizinate on an IL-4- and IL-13-induced atopic dermatitis-like skin-equivalent model, *Arch. Dermatol. Res.*, 2019, **311**, 131–140.
- 38 F. Tanaka, M. Uda, Y. Hirose and Y. Hirai, Restoration of calcium-induced differentiation potential and tight junction formation in HaCaT keratinocytes by functional attenuation of overexpressed high mobility group box-1 protein, *Cytotechnology*, 2020, **72**, 165–174.
- 39 Y. Li, T. Liu, C. Yan, R. Xie, Z. Guo, S. Wang, Y. Zhang, Z. Li, B. Wang and H. Cao, Diammonium Glycyrrhizinate Protects against Nonalcoholic Fatty Liver Disease in Mice through Modulation of Gut Microbiota and Restoration of Intestinal Barrier, *Mol. Pharm.*, 2018, **15**, 3860–3870.

Keywords

absorption enhancer; docking; epithelial cell; glycyrrhizin; nuclear magnetic resonance (NMR); PDZ domain; tight junction; TrNOE; zonula occludens-1

Data availability

All data described in the article are contained within the article.

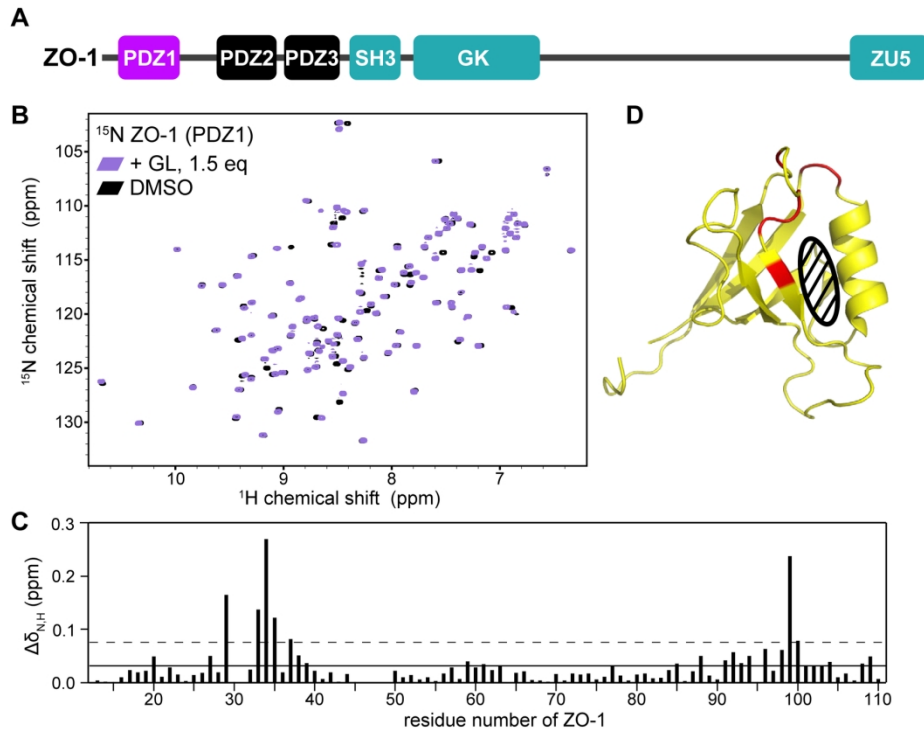
Supplementary information

This article contains supplementary information.

Funding and additional information

This work was supported in part by the Japan Science and Technology Agency, A-step Feasibility Study Program (AS262Z01275Q, AS242Z00566Q), Japan Society for the Promotion of Science KAKENHI (15H04337), AMED Translational Research Program, and Strategic PRomotion for practical application of INnovative medical Technology (TR-SPRINT) under Grant Number 20lm0203011-j0002.

Figure 1

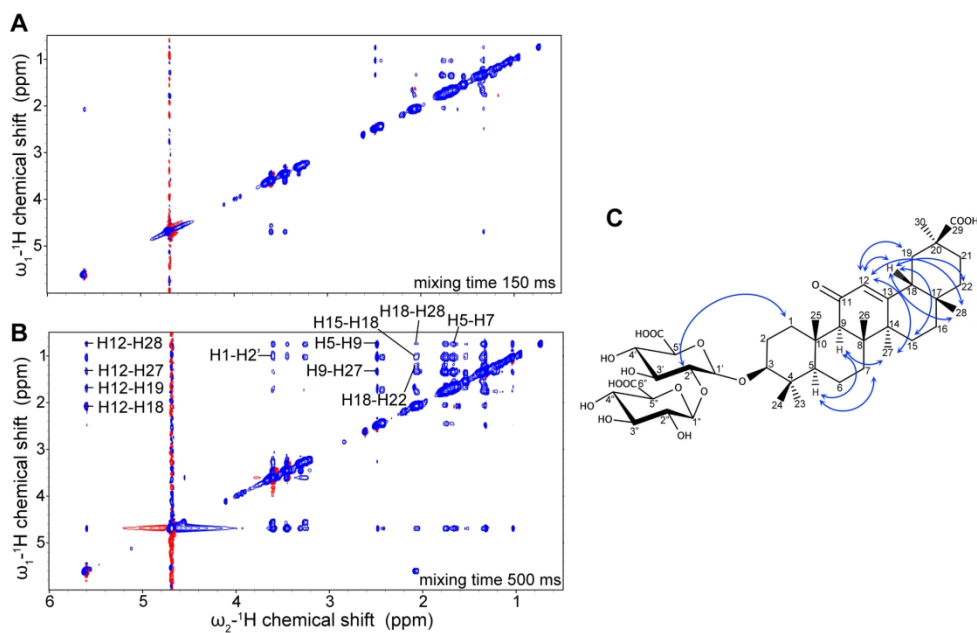


Identification of the key residues of the ZO-1(PDZ1) domain responsible for GL recognition.

- A. Domain architecture of human ZO-1. PDZ, PDZ domain; SH3, Src homology 3 domain; GK, guanylate kinase domain; ZU5, ZO-1, and UNC5 domain.
- B. Overlaid two-dimensional ^1H - ^{15}N HSQC spectra of ZO-1(PDZ1) with (red) and without (black) GL.
- C. Normalized chemical shift change of the ZO-1(PDZ1) domain upon mixing with the 1.5 equivalence of GL.
- D. The residues with larger chemical shift changes than the threshold values are mapped onto the NMR structure of ZO-1(PDZ1) (PDB: 2rrm, chain A) colored in red. The threshold value is indicated by the dashed line in graph C. The black diagonal area shows the canonical binding pocket of the PDZ domain.

165x142mm (300 x 300 DPI)

Figure 2

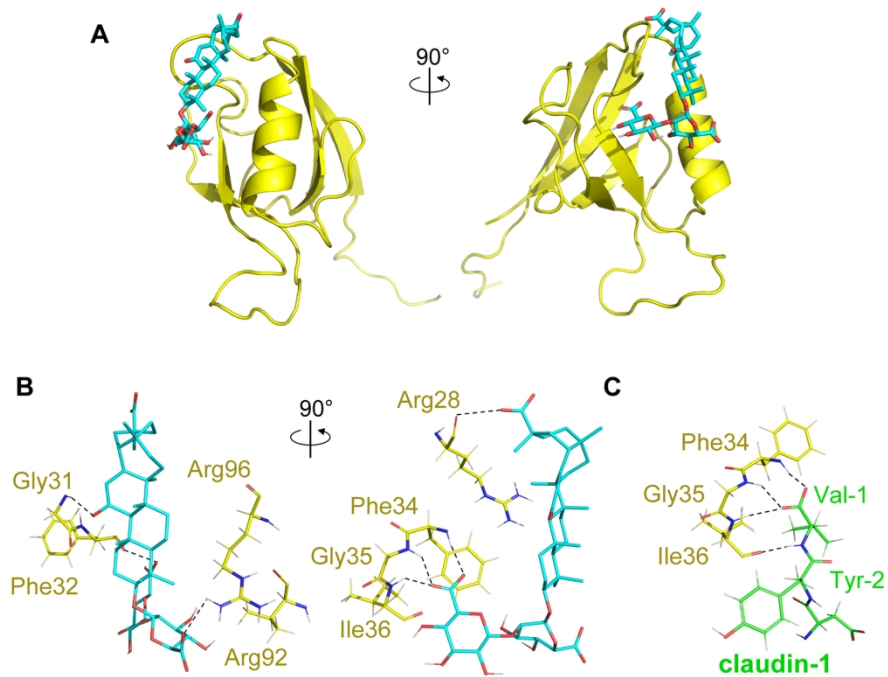


2D ^1H - ^1H NOESY spectra of GL at 2 mM in the presence of ZO-1(PDZ1).
 A, B. NMR measurement using 150-ms (A) and 500-ms (B) mixing time, respectively. Blue and red indicate the same and opposite sign as the diagonal peak, respectively. The assigned NOE peaks were used for the docking.

C. Chemical structure of GL and pairs of hydrogens with NOE peaks observed used for docking.

170x135mm (300 x 300 DPI)

Figure 3



HADDOCK structure with the highest score.

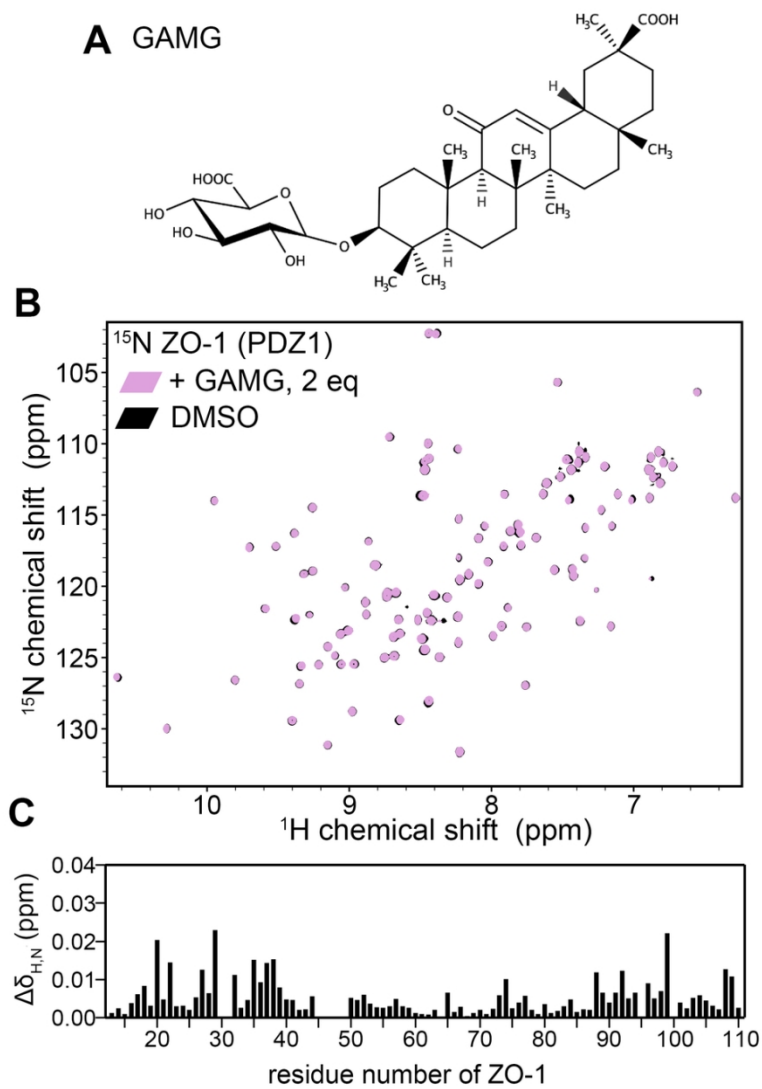
A. The overall structure. ZO-1(PDZ1) is coloured in yellow and GL in cyan.

B. The enlarged view of the binding sites is shown. The dashed lines represent hydrogen bonds.

C. X-ray structure of ZO-1(PDZ1) and the C-terminal tail of claudin-1 from 4OEP. ZO-1(PDZ1) is coloured in yellow and claudin-1 in light green.

162x135mm (300 x 300 DPI)

Figure 4



No binding between ZO-1(PDZ1) and GAMG was detected.

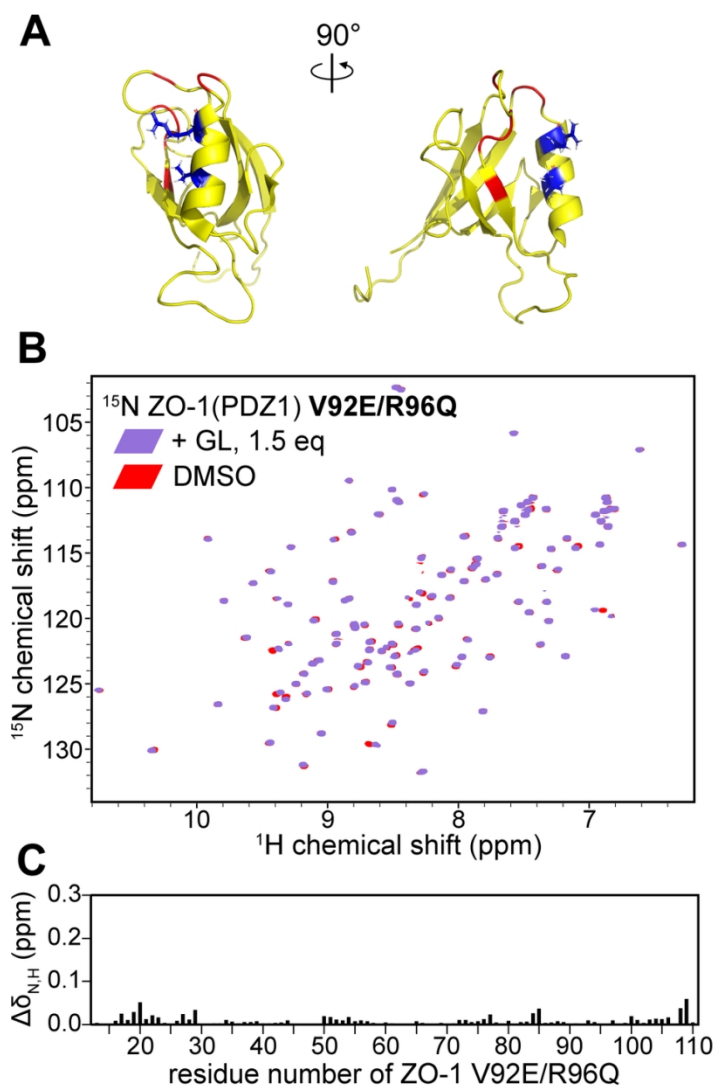
A. The chemical structure of GAMG.

B. HSQC spectra of ZO-1(PDZ1) with and without two equivalents of GAMG.

C. The chemical shift change.

82x128mm (300 x 300 DPI)

Figure 5



No binding between ZO-1(PDZ1) mutant and GL was detected.

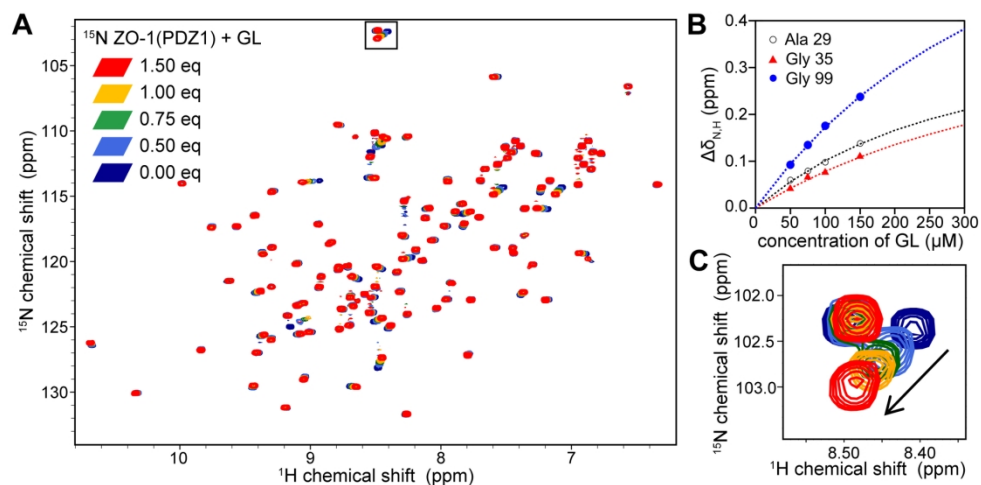
A. The mutated residues are shown on the steric structure. Red and blue represent the residues that showed significant CSP as shown in Fig. 1D and the residues where the mutations were introduced, respectively.

B. HSQC spectra of ZO-1(PDZ1) V92E/R96Q mutant with and without 1.5 equivalents of GL.

C. The chemical shift change. Vertical axis scale is the same as in Fig. 1C.

82x136mm (300 x 300 DPI)

Figure 6

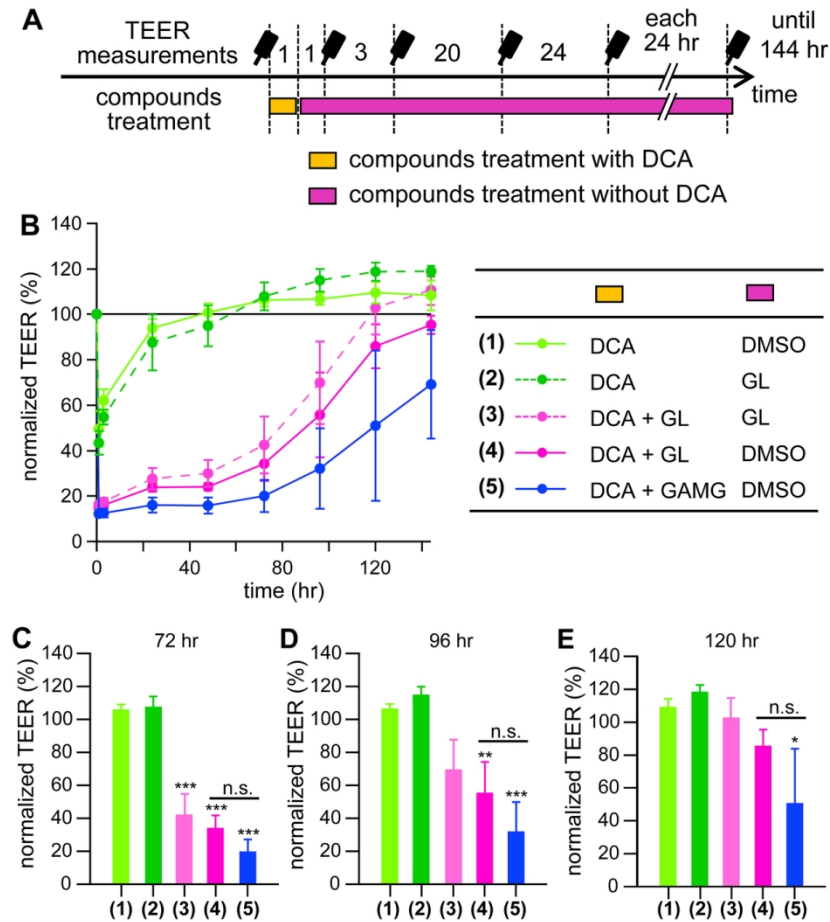


NMR titration experiments for ZO-1(PDZ1) with GL.

- A. Overlaid spectra of ^{15}N -ZO-1(PDZ1) with GL of 0, 0.5, 0.75, 1, and 1.5 equivalents. Note that Fig. 1B shows the overlaid spectrum of two spectra with GL of 0 and 1.5 equivalents.
- B. Best fit dissociation constant curves. Residues Ala29, Gly35, and Ser98 are shown.
- C. The peak shifting of Gly98 is shown as an example.

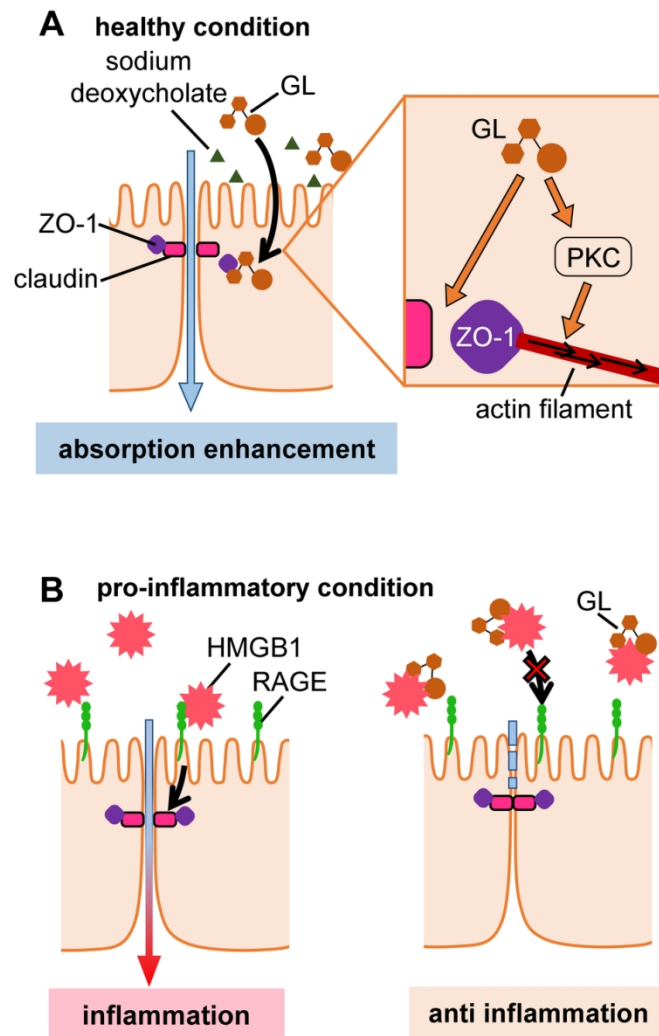
170x112mm (300 x 300 DPI)

Figure 7



Caption : TEER changes in Caco-2 cells. A. Experimental procedures. Yellow and pink arrows indicate the first administration and the second and subsequent administrations, respectively. Details of the timing of TEER measurement compound administration are described in the experimental procedures. Each point represents mean \pm s.d. ($n=3$). B. Time course of TEER normalized to 100% of TEER before the initial administration. C-E Bar graphs extracted from B for 72hr (C), 96hr (D), and 120hr (E) time points. Multiple comparison tests were performed for each time point. The data were analysed by one-way ANOVA using Tukey post hoc tests ($\alpha = 0.05$). "*" indicates p -value < 0.5 , ** indicates p -value < 0.1 , and *** indicates p -value < 0.001 for comparison with (1). Comparing (4) and (5), there was no significant difference. "n.s." means no significant difference.

Figure 8



Scheme of the effects of GL.

A. GL opens TJs in two ways: contraction of actin via the PKC pathway and binding to ZO-1, which has a pro-absorption effect.

B. In the case of inflammation, GL binds to the released HMGB1 and shows an anti-inflammatory effect.

82x145mm (300 x 300 DPI)